

**Orientation-position coupling in the two-dimensional XY model**Zhufei Xiao (肖竹飞), Tao Huang (黄韬), and Chunhua Zeng (曾春华)<sup>\*</sup>*Faculty of Science/Faculty of Information Engineering and Automation, Kunming University of Science and Technology, Kunming 650500, People's Republic of China*

(Received 13 March 2024; revised 30 May 2024; accepted 20 June 2024; published 17 July 2024)

The XY model is a valuable tool for analyzing spin systems. While the two-dimensional (2D) classical XY model and its variations that only consider spin interactions have been extensively studied, limited exploration has been conducted on the 2D XY model with orientation-position coupled (OPC) interactions. In the present study, we extend the 2D classical XY model by making the exchange energy dependent on the spin position; this model is referred to as the 2D compressible XY (CXY) model. Compared to the 2D classical XY model, we find that the OPC interaction enhances the stability of the orientational structure of the system. The deformation induced effects on the rotational degrees of freedom of the system indicates that the increase in the stretching deformation enhances the orientational order of spins. Furthermore, the coupling between orientation and position is demonstrated by calculating the joint probability distribution of spin orientation and position fluctuations. This study advances comprehension of spin systems' elasticity and provides new ideas for controlling the stability of the orientational order of spin systems.

DOI: [10.1103/PhysRevB.110.024312](https://doi.org/10.1103/PhysRevB.110.024312)**I. INTRODUCTION**

The XY model has been extensively studied in the fields of statistical physics and condensed matter physics, yielding fruitful results both theoretically and experimentally [1–3]. Notably, since Berezinskii [4], Kosterlitz [5,6], and Thouless [5] discovered topological defects and unconventional phase transitions in the two-dimensional (2D) classical XY model, numerous research papers have explored phase transitions and critical phenomena in similar models. In recent years, the 2D classical XY model and its extensions have remained an active area of research. For example, researchers have utilized a nonequilibrium expansion of the XY model to investigate the static and dynamic properties of vortices and the effect of self-spinning on the Berezinskii-Kosterlitz-Thouless phase transition scenario [7]. Machine learning techniques have been employed to identify the XY model's phases structure and phase transitions [8–10]. Vision cone interactions have also been introduced in the XY model with short-range coupling, revealing an accurate long-range ordered phase where the directed propagation of defects disrupts the parity and time-reversal symmetry of spin dynamics [11]. These studies related to the XY model and its extensions have considered only spin interactions.

It is widely acknowledged that orientation-position coupling (OPC) are prevalent in nature, impacting various physical properties and dynamic behaviors of systems, such as the phase behaviors [12–14], thermodynamic properties [15], material microstructure [16], etc. Previous studies have investigated similar scenarios, such as spin-lattice coupling [16–19], spin-phonon coupling [20,21], magnetoelastic interactions

[22–24], the compressible Ising model [12,25,26], and the Doye model [27]. Among these, the compressible Ising model, introduced by Landau *et al.*, exhibits phase separation when the exchange energy between spins influenced by the elastic interaction in a Lennard-Jones-like way [12]. The Doye model, comprising a Lennard-Jones-like potential and an anisotropic factor, offers insights into the phase transition of 2D crystal composed of Janus colloidal particles. Elastic effects within the Doye model lead to a first-order solid-solid transition within the system [28,29]. Therefore, it is highly important to consider the OPC, i.e., the lattice deformations in spin systems. Recently, the coupling of the XY model and the Fermi-Pasta-Ulam-Tsingou  $\beta$  model, a compressible XY model, has been used to study heat conduction in a 1D chain of particles with OPC interaction [30]. At low temperatures, the OPC interaction reduces the thermal conductivity of the translational degrees of freedom and makes the thermal conduction different between translational and rotational degrees of freedom.

In real spin systems, it is imperative to consider elastic interactions. This research focuses on studying lattice deformation effects in a 2D spin-lattice system with OPC. To accommodate OPC, we extend the XY model by incorporating a position-dependent exchange energy, similar to approaches seen in the compressible Ising and Doye models, resulting in the 2D compressible XY (CXY) model. We employ molecular dynamics methods to simulate both the XY and CXY models under equilibrium condition. We find that OPC interaction enhances the orientational order of the spins. OPC interaction causes a rise in the distances between nearest-neighbor spins within the system. Moreover, compression and stretching of the CXY model are simulated by adjusting the lattice constants  $a$ . We find that, as long as the lattice structure remains intact, the stability of the orientational

<sup>\*</sup>Contact author: [zchh2009@126.com](mailto:zchh2009@126.com)

structure is enhanced during lattice stretching. Additionally, we explore the coupling effects between spin orientation and position by calculating the joint probability density distribution of spin orientation and position fluctuations.

The paper is structured as follows: In Sec. II, the model, simulation method, and parameter settings are presented in detail. In Sec. III we show the numerical results and conducts a detailed analysis. The last section summarizes the findings and offers a discussion in the importance of considering OPCs in spin systems.

## II. MODEL AND SIMULATION METHODS

In this context, we extend the ferromagnetic XY model on the square lattice to include the OPC interaction, taking cues from both the compressible Ising model [12,15,26] and the Doye model [28,29]. The pair interaction  $\Phi_{ij}$  between two neighboring spins,  $i$  and  $j$ , is

$$\Phi_{ij}(r_{ij}, \theta_i, \theta_j) = f(\theta_i, \theta_j)U(r_{ij}). \quad (1)$$

In Eq. (1), the orientation-dependent factor  $f$  takes the form of the XY model

$$f(\theta_i, \theta_j) = A - J\cos(\theta_i - \theta_j), \quad (2)$$

where  $J$  is the coupling constant and  $\theta_i$  is the orientation of the  $i$ th spin. The position-dependent factor  $U$  takes the form of the Lennard-Jones (LJ) potential

$$U_{LJ}(r_{ij}) = 4\epsilon \left[ \left( \frac{\sigma}{r_{ij}} \right)^{12} - \left( \frac{\sigma}{r_{ij}} \right)^6 \right] + B, \quad (3)$$

where  $r_{ij}$  is the distance between the nearest-neighboring spins  $i$  and  $j$ ,  $\sigma$  represents the characteristic length in the spin interaction, and  $\epsilon$  indicates the depth of the potential well. Similar to the 2D compressible Ising model, the model described by Eq. (1) can be referred to as the 2D CXY model. For theoretical exploration, we introduce constants  $A$  and  $B$ , setting values that are not too small, such as  $A = 40$  and  $B = 2.0$ . On the one hand, a sufficiently large  $A$  can increase the well depth of the LJ potential, allowing the system to maintain its lattice structure within the simulated temperature range. On the other hand, a  $B$  value exceeding 1.0 ensures that the potential energy minimum of the LJ potential remains positive, ensuring the behavior of the spin system as a ferromagnetic system.

Rather than employing the Monte Carlo method [11,31,32], tensor renormalization group [33] or tensor networks [34] to study the XY model, we aim to examine the spin system based on its dynamical details. So, we implement the molecular dynamics simulation [28,35] of the CXY model by introducing the kinetic energy term. The Hamiltonian of the CXY model is defined as

$$H = \sum_{i,j} \left[ \frac{1}{2}m\mathbf{v}_i^2 + \frac{1}{2}I\omega_i^2 + \Phi_{ij} \right], \quad (4)$$

where the sum runs over all nearest-neighboring lattice sites of  $i$ .  $\mathbf{v}_i$  represents the velocity vector of the spins' translational degrees of freedom.  $\omega_i$  denotes the angular velocity of the spins. The first two terms within the summation on the right-hand side of Eq. (4) correspond to the translational and

rotational kinetic energies, respectively. The  $NVT$  ensemble of the solid state of the CXY model is simulated using periodic boundary conditions and a Langevin thermostat [36]. The equations of motion governing the system are given by

$$\begin{aligned} \dot{\mathbf{x}}_i &= \mathbf{v}_i, & \dot{\theta}_i &= \omega_i, \\ m\dot{\mathbf{v}}_i &= -\frac{\partial H}{\partial \mathbf{x}_i} + (-\lambda_t \mathbf{v}_i + \xi_i)\delta_i, \\ I\dot{\omega}_i &= -\frac{\partial H}{\partial \theta_i} + (-\lambda_r \omega_i + \eta_i)\delta_i, \end{aligned} \quad (5)$$

where  $i = 1, 2, \dots, L^2$  ( $L = 128$ ).  $\xi_i$  and  $\eta_i$  denote Gaussian white noise and satisfy

$$\begin{aligned} \langle \xi_i \rangle &= 0, & \langle \eta_i \rangle &= 0, \\ \langle \xi_i(t)\xi_i(t') \rangle &= 2\lambda_t k_B T_i \delta(t - t'), \\ \langle \eta_i(t)\eta_i(t') \rangle &= 2\lambda_r k_B T_i \delta(t - t'), \end{aligned} \quad (6)$$

where  $\langle \dots \rangle$  represents the ensemble average, and  $\lambda_t$ ,  $\lambda_r$  are the coupling strengths of the system's translational and rotational degrees of freedom to the heat bath, respectively. Throughout the simulation, we set dimensionless unit mass  $m$ , rotational inertia  $I$ , and the Boltzmann constant  $k_B$  to 1.0 for simplicity, resulting in temperature being expressed in energy units.  $T_i$  denotes the temperature of the heat bath.

In the simulations, we use the second-order BAOAB algorithm [37] with a time step of  $\Delta t = 0.005$  to solve the stochastic differential equations in Eq. (5). We use a homemade CUDA program to perform molecular dynamics simulations on GPUs. In the system's initial state, we initialize the distance  $r_{ij} = aD$  ( $a = \sqrt[6]{2}\sigma$  is the equilibrium distance, while  $D$  denotes the compression ratio) and  $\theta_i = 0$  for all spins. A simulation is performed at each temperature  $T$  and compression ratio  $D$ , with the system eventually reaching an equilibrium state following a sufficiently long relaxation time. All the statistics and analysis are then performed on the system in this equilibrium state. Extra tests ensure that the current system is large enough with no obvious finite-size effects.

## III. RESULTS

The XY model exhibits a Berezinskii-Kosterlitz-Thouless phase transition [4–6,38], transitioning from a quasicrystalline phase to a disordered phase as temperature rises, accompanied by the decoupling of vortex pairs. In the absence of an external magnetic field, the spontaneous magnetization [11] serves as an order parameter of the XY model, delineating the shift from a low-temperature quasicrystalline state to a high-temperature disordered state. The spontaneous magnetization is described by

$$M = \frac{\sqrt{(\sum \cos\theta_i)^2 + (\sum \sin\theta_i)^2}}{L^2}, \quad (7)$$

where the sum runs over all lattice sites, and  $L^2$  denotes the size of the system. Spontaneous magnetization susceptibility

$$\chi = \langle M^2 \rangle - \langle M \rangle^2, \quad (8)$$

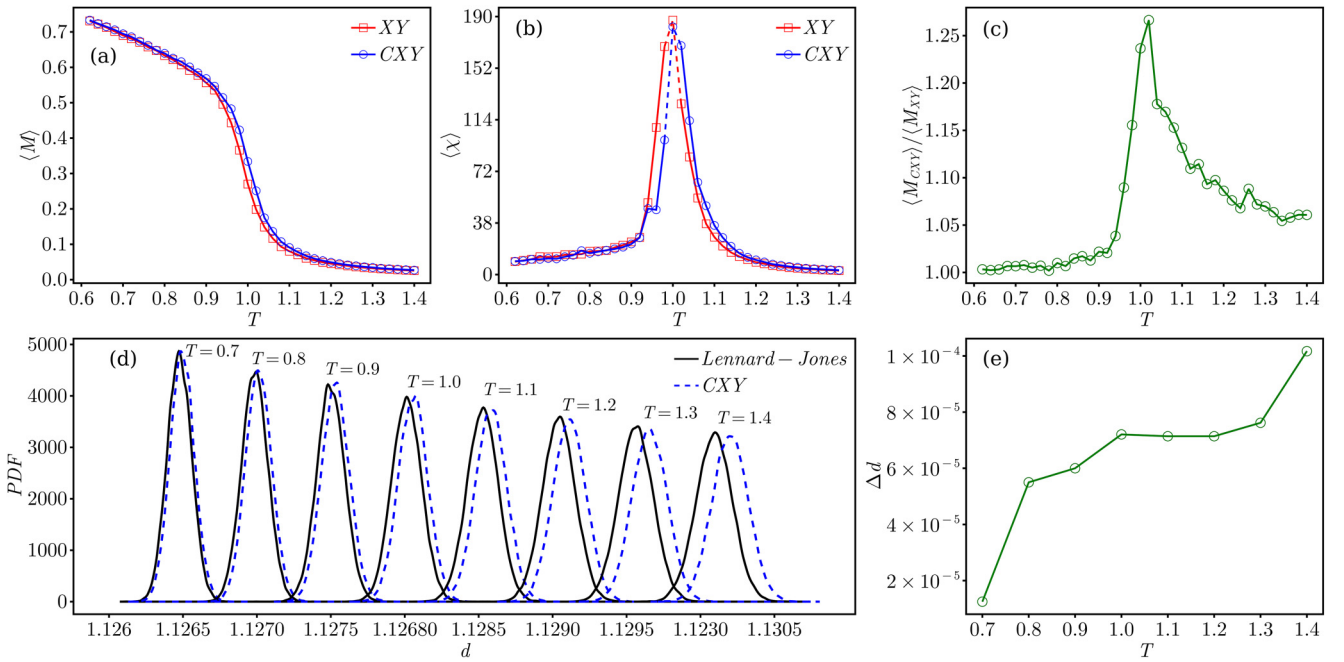


FIG. 1. (a) Average of spontaneous magnetization  $\langle M_{XY} \rangle$  (red) and  $\langle M_{CXY} \rangle$  (blue) as function of  $T$ . (b) The spontaneous magnetization susceptibility  $\langle \chi_{XY} \rangle$  (red) and  $\langle \chi_{CXY} \rangle$  (blue) as function of  $T$ . (c) The dependence of  $\langle M_{CXY} \rangle / \langle M_{XY} \rangle$  on  $T$ . (d) The probability density distribution of the mean distance between spins at different temperatures ranges from 0.7 to 1.4 with 0.1 increments. The solid and dashed lines represent the LJ potential and the CXY model, respectively. (e) The ratio of the means of the two sets of probability density distributions in (d) as function of  $T$ .

with a sharp peak occurring close to the critical point. For comparison with the XY model, we employ both Eqs. (7) and (8) to measure the transition of the orientational structure from a low-temperature quasicrystalline state to a high-temperature disordered state in the CXY model.

The average spontaneous magnetization  $\langle M \rangle$  per spin and the spontaneous magnetization susceptibility  $\chi$ , against temperature  $T$ , are illustrated in Figs. 1(a) and 1(b), respectively. Averages  $\langle \cdot \rangle$  are taken over all spins and multiple realizations in the same set of parameters. In Figs. 1(a) and 1(b), the temperature dependence of  $\langle M \rangle$  and  $\chi$  for both the XY model and the CXY model indicates transitions occurring within a finite temperature range. However, the curves for the two models do not overlap in either Figs. 1(a) or 1(b), and all values of  $\langle M_{CXY} \rangle / \langle M_{XY} \rangle$  greater than 1.0 persist even when the system orientation approaches disorder, reaching a maximum value of 1.266 [as depicted in Fig. 1(c)] at  $T = 1.04$ . This suggests the presence of other ordered structures in the CXY model, such as more extensive orientation spatial correlations. We corroborated that the CXY model exhibits more extended orientation spatial correlation than the XY model by calculating the spin-spin spatial correlation function (illustrated in Fig. 2). Additionally, in Fig. 2(b), although the peak for the spontaneous magnetic susceptibility for both the CXY model and the XY model occurs at  $T \approx 1.0$ , the trend of the curves shows that in simulations with denser temperature points, the peak of the spontaneous magnetic susceptibility of the CXY model is observed at a higher temperature compared to that of the XY model. This can be attributed to OPC interaction enhancing the stability of the orientational structure within the system, resulting in a higher critical temperature. Furthermore,

the probability density distribution of the average distance between nearest-neighbor spins in the CXY model and the LJ potential are calculated and depicted in Fig. 1(d), respectively. Figure 1(e) illustrates how the ratio of the mean values of  $d$

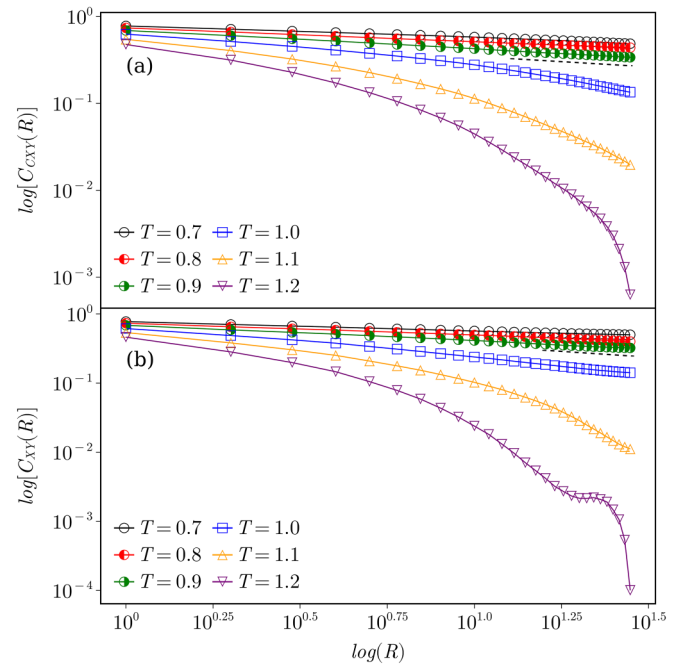


FIG. 2. Decay of spin-spin spatial correlation functions  $\langle C_\theta(R) \rangle$  (in log-log) with  $R$  at different temperatures. (a) and (b) denote the decay of  $\langle C_{CXY}(R) \rangle$  and  $\langle C_{XY}(R) \rangle$ , respectively.

for the two models at the same temperature in Fig. 1(d) varies with temperature. Figures 1(d) and 1(e) show that at the same temperature, the average distance of the nearest-neighboring spins for the CXY model is larger than that of the LJ potential, and the ratio between the two increases with increasing temperature. The two phenomena mentioned above can be attributed to OPC interaction, which produce more dispersion at distances between the nearest-neighboring spins than does the LJ potential as the temperature increases.

To further investigate the effect of OPC interaction on the rotational degrees of freedom, we study the spin-spin spatial correlation function defined as

$$\langle C_\theta(R) \rangle = \langle \cos[\theta_i(0) - \theta_j(R)] \rangle, \quad (9)$$

which is plotted in Fig. 2.  $R$  is the distance between the  $i$ th spin and the  $j$ th spin. Figures 2(a) and 2(b) show the spin-spin spatial correlation functions of the CXY model and XY model, respectively. When comparing these figures, both the CXY model and the XY model exhibit quasi-long-range ordering, characterized by an algebraically decaying spin-spin spatial correlation function at low temperatures and a completely disordered phase with an exponentially decaying spin-spin spatial correlation function at high temperatures. Although the spin-spin spatial correlation functions of the CXY model and the XY model decay similarly, the correlation function of the CXY model declines at a slower rate than that of the XY model. This finding suggests that the CXY model has a stronger orientational correlation, explaining why the CXY model is more ordered than the XY model at the same temperature, even when the system's orientation is approaching disorder [as demonstrated in Figs. 2(a), 2(b), and 2(c)].

Systems in nature are subject to various external influences, such as deformation caused by tension or pressure. Introducing OPC enables us to examine the behavior of the orientational structure under system deformation by altering the lattice constant. The lattice constant  $a = a_0 D$  is varied, in which  $a_0 = \sqrt{2}\sigma$  is the initial distance between the nearest-neighboring spins in the system, and  $D = 0.99, 1.0, 1.005, 1.01, 1.015, 1.02, 1.025, 1.03$  as the compression ratios.  $D < 1.0$  indicates that the system is compressed, while  $D > 1.0$  indicates that the system is stretched.

Figure 3 shows how  $\langle M \rangle$  and  $\langle M_D \rangle / \langle M_{1.0} \rangle$  depend on the compression ratios  $D$  and temperatures  $T$ . When the system undergoes a 1% compression, the profile of the system's spontaneous magnetization versus temperature closely resembles that without compression. This alignment corresponds to the temperature dependence of the system energy and the probability density distribution between average distance of the nearest-neighbor spins at  $D = 0.99$  (as depicted in Fig. 4). After compression, as the system reaches an equilibrium state, the average distances between the nearest-neighboring spins closely approximate those at  $a = 0.99a_0$ . Consequently, an energy competition between the translational and rotational degrees of freedom emerges, which closely mirrors that in the absence of compression, resulting in a spontaneous magnetization that exhibits minimal differences. However, for the stretching scenario, the behavior of spontaneous magnetization differs. It increases with a rising compression ratio  $D$  at the same temperature. Furthermore, at the same compression ratio,  $\langle M_D \rangle / \langle M_{1.0} \rangle$  first increases and

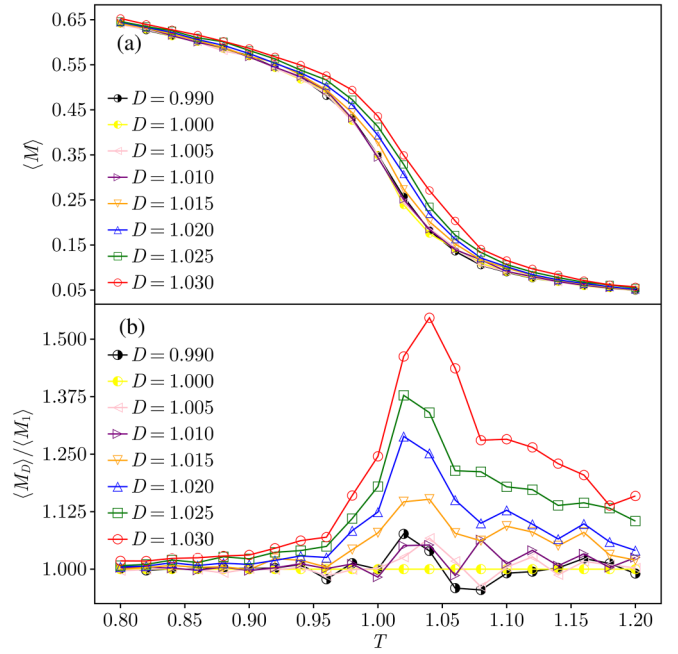


FIG. 3. Average of spontaneous magnetization of CXY model as function of  $T$  and  $D$ . (a) and (b) denote the  $\langle M \rangle$  and  $\langle M_D \rangle / \langle M_{1.0} \rangle$ , respectively.

then decreases with increasing temperature. This observation suggests that the stretching system can enhance its stability of the orientational structure and its tolerance to temperature fluctuations.

To delve deeper into the coupling between orientation and position, we computed the orientation fluctuation  $\Delta\theta_i = \theta_i - \langle \theta_i \rangle$ , and the position fluctuation  $\Delta x_i = x_i - \langle x_i \rangle$ .

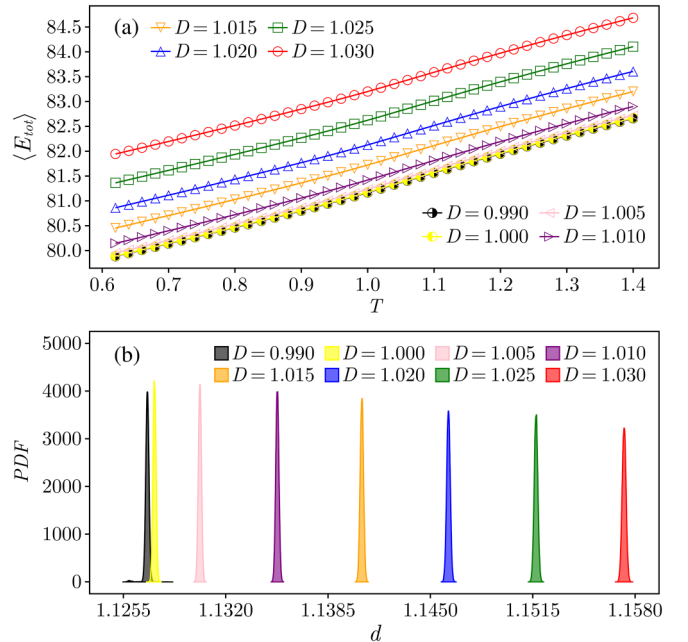


FIG. 4. (a) The per spin energy as function of  $T$  and  $D$ . (b) The probability density distribution of the average distance between nearest-neighbor spins at  $T = 1.0$  and  $D$  from 0.99 to 1.03.

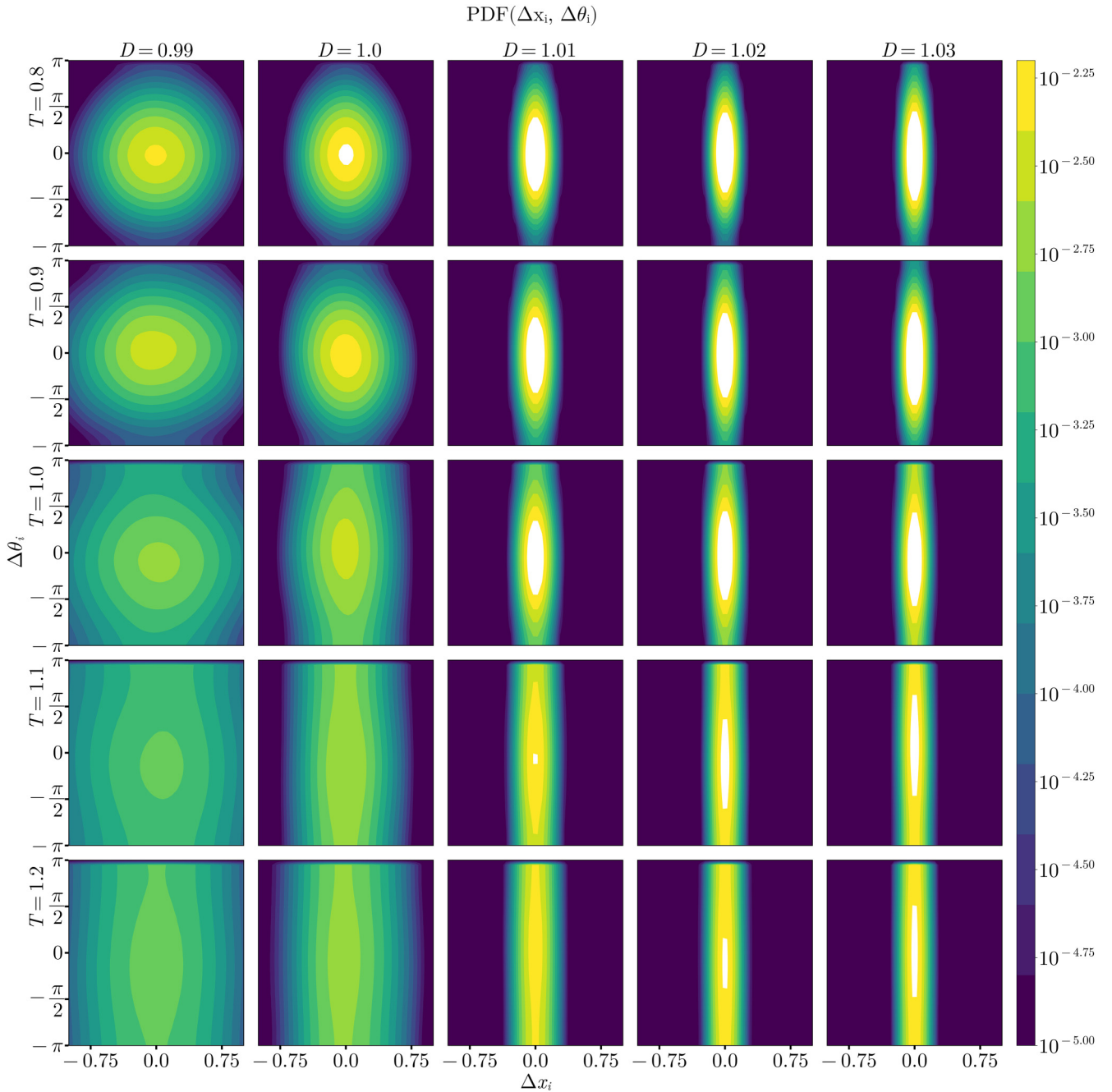


FIG. 5. The joint probability density distributions of the spin orientation fluctuation  $\Delta\theta_i$  and position fluctuation  $\Delta x_i$ . Rows: The  $PDF(\Delta\theta_i, \Delta x_i)$  as function of  $D$ . Columns: The  $PDF(\Delta\theta_i, \Delta x_i)$  as function of  $T$ .

Subsequently, we calculated the joint probability density distributions of  $\Delta\theta_i$  and  $\Delta x_i$ , and the results are depicted in Fig. 5. In Fig. 5, each column and row illustrate the variations in the joint probability density distribution between  $\Delta\theta_i$  and  $\Delta x_i$  with the system temperature  $T$  and the compression ratio  $D$ , respectively. For each column in Fig. 5, the nonuniformity of the joint probability density distribution between  $\Delta\theta_i$  and  $\Delta x_i$  decreases with increasing  $T$ , indicating that the correlation between  $\Delta\theta_i$  and  $\Delta x_i$  is weakened. This phenomenon arises because, at different compression ratios [as illustrated in Fig. 3(a)], the system's orientational structure consistently transition from a quasicrystalline state at low temperatures to a disordered state at high temperatures.

Consequently, as temperature increases, the orientations of all spins in the system become more uniformly distributed in  $(-\pi, \pi]$ . Concurrently, within each row of Fig. 5, the probability density distribution becomes more and more concentrated as the compression increases, indicating a stronger correlation between  $\Delta\theta_i$  and  $\Delta x_i$ . From Fig. 5 ( $T = 1.0$  and  $D = 1.0, 1.01$ ), smaller  $\Delta\theta_i$  appears with higher probability as the system is stretched, which means that the orientational degrees of freedom of the system has a higher order (consistent with the findings in Fig. 3). This enhancement results from the OPC, i.e., correlation of  $\Delta x_i$  and  $\Delta\theta_i$  in energy. In the joint probability density distribution of the first three rows of Fig. 5, the equal probability lines are elliptical, indicating that  $\Delta x_i$

and  $\Delta\theta_i$  are not independent. When the system is stretched, the translational degrees of freedom reach a higher energy level and the range of translational vibrations decreases. Therefore,  $\Delta\theta_i$  will change depending on the relationship between  $\Delta x_i$  and  $\Delta\theta_i$ . These factors contribute to a more irregular joint probability density distribution of  $\Delta\theta_i$  and  $\Delta x_i$ ; more uneven.

#### IV. CONCLUSION AND DISCUSSION

In this study, we extend beyond the classical XY model and its extensions, which solely consider spin interaction, by incorporating OPC to examine the impact of lattice deformation on the spin system. Results from our molecular dynamics simulations show that the orientational structure of the CXY model exhibits greater stability compared to that of the XY model. This stability is observed to increase with the stronger extensive spin-spin spatial correlation due to the scratching deformation of the system. Our findings suggest that systems incorporating OPC display a more complicated phase structure and dynamic behavior compared to those considering only rotational degrees of freedom. For example, the Doye model describes a patch colloidal particle system that undergoes a solid-solid phase transition [28]. The spin-lattice coupling in paramagnetic materials  $C_r N$  causes nonadiabatic effects, which shorten the lifetime of phonons at low temperatures [39]. The coupling of electromagnetic interaction and elastic interaction in the metamaterial lattice allows the electromagnetic induction force to change the structure of the metamaterial and dynamically adjust its effective properties [40]. The compressibility's influence can modify the domain growth exponent, leading to phase separation in the compressible Ising model [12]. These findings underscore the importance of considering OPC in spin systems.

Elastic interactions are common in many real spin systems and are susceptible to external forces (e.g., tension and pressure). We use molecular dynamics simulation to study the CXY model with OPC interaction. This exploration enhances our understanding of how elastic effects emerge in spin systems. Moreover, our key finding is the significant influence of lattice's stretching deformation on the stability of orientational structure in the CXY model. This conclusion suggests that we can manipulate the stability of orientational structure through external stress to enhance its temperature tolerance because external stress can induce the deformation of the spin lattice. This insight motivates us to consider spin's orientation-position coupling in various spin systems (such as the magnetic skyrmions system [41–43]), and to try to adjust the stability of the orientational structure by manipulating external stresses. Furthermore, the coupling form described in Eq. (1) in this study demonstrates that multiplying the LJ potential on  $J$  is equivalent to changing the temperature scale of the rotational degrees of freedom of the XY model; thus, leading to the results obtained in this study. For more complex coupling methods, such as direct coupling of particle orientation and position [28,29], the system may exhibit even more intriguing and diverse physical properties.

#### ACKNOWLEDGMENTS

This work was funded by the National Natural Science Foundation of China (Grants No. 12265017 and No. 12247205), Yunnan Fundamental Research Projects (Grants No. 202201AV070003 and No. 202101AS070018), Yunnan Province Ten Thousand Talents Plan Young and Elite Talents Project and Yunnan Province Computational Physics and Applied Science and Technology Innovation Team.

Z.X. and T.H. contributed equally to this work.

- 
- [1] Z. Gulácsi and M. Gulácsi, Theory of phase transitions in two-dimensional systems, *Adv. Phys.* **47**, 1 (1998).
  - [2] J. Struck, M. Weinberg, C. Ölschläger, P. Windpassinger, J. Simonet, K. Sengstock, R. Höppner, P. Hauke, A. Eckardt, M. Lewenstein, and L. Mathey, Engineering Ising-XY spin-models in a triangular lattice using tunable artificial gauge fields, *Nat. Phys.* **9**, 738 (2013).
  - [3] N. G. Berloff, M. Silva, K. Kalinin, A. Askitopoulos, J. D. Töpfer, P. Cilibrizzi, W. Langbein, and P. G. Lagoudakis, Realizing the classical XY Hamiltonian in polariton simulators, *Nat. Mater.* **16**, 1120 (2017).
  - [4] V. L. Berezinskii, Destruction of long-range order in one-dimensional and two-dimensional systems having a continuous symmetry group I. Classical systems, *Zh. Eksp. Teor. Fiz.* **59**, 907 (1970) [*Sov. Phys. JETP* **32**, 493 (1971)].
  - [5] J. M. Kosterlitz and D. J. Thouless, Ordering, metastability and phase transitions in two-dimensional systems, *J. Phys. C* **6**, 1181 (1973).
  - [6] J. M. Kosterlitz, The critical properties of the two-dimensional xy model, *J. Phys. C* **7**, 1046 (1974).
  - [7] Y. Rouzair and D. Levis, Defect superdiffusion and unbinding in a 2D XY model of self-driven rotors, *Phys. Rev. Lett.* **127**, 088004 (2021).
  - [8] J. F. Rodríguez-Nieva and M. S. Scheurer, Identifying topological order through unsupervised machine learning, *Nat. Phys.* **15**, 790 (2019).
  - [9] C.-H. Song, Q.-C. Gao, X.-Y. Hou, X. Wang, Z. Zhou, Y. He, H. Guo, and C.-C. Chien, Machine learning of the XY model on a spherical Fibonacci lattice, *Phys. Rev. Res.* **4**, 023005 (2022).
  - [10] W. Zhang, J. Liu, and T.-C. Wei, Machine learning of phase transitions in the percolation and XY models, *Phys. Rev. E* **99**, 032142 (2019).
  - [11] S. A. M. Loos, S. H. L. Klapp, and T. Martynec, Long-range order and directional defect propagation in the nonreciprocal XY model with vision cone interactions, *Phys. Rev. Lett.* **130**, 198301 (2023).
  - [12] S. J. Mitchell and D. P. Landau, Phase separation in a compressible 2D Ising model, *Phys. Rev. Lett.* **97**, 025701 (2006).
  - [13] A. Paul, C.-M. Chung, T. Birol, and H. J. Changlani, Spin-lattice coupling and the emergence of the trimerized phase in the  $S = 1$  kagome antiferromagnet, *Phys. Rev. Lett.* **124**, 167203 (2020).
  - [14] A. Orendáčová, R. Tarasenko, V. Tkáč, E. Čížmár, M. Orendáč, and A. Feher, Interplay of spin and spatial anisotropy in low-dimensional quantum magnets with spin 1/2, *Crystals* **9**, 6 (2018).

- [15] T. Balcerzak, K. Szałowski, and M. Jaščur, Thermodynamic properties of the one-dimensional Ising model with magnetoelastic interaction, *J. Magn. Magn. Mater.* **507**, 166825 (2020).
- [16] G. Qin, H. Wang, L. Zhang, Z. Qin, and M. Hu, Giant effect of spin–lattice coupling on the thermal transport in two-dimensional ferromagnetic, *J. Mater. Chem. C* **8**, 3520 (2020).
- [17] K. Aoyama and H. Kawamura, Spin-lattice-coupled order in Heisenberg antiferromagnets on the pyrochlore lattice, *Phys. Rev. Lett.* **116**, 257201 (2016).
- [18] Y. Wu, H. Wen, W. Chen, and Y. Zheng, Microdynamic study of spin-lattice coupling effects on skyrmion transport, *Phys. Rev. Lett.* **127**, 097201 (2021).
- [19] S. Mankovsky, S. Polesya, H. Lange, M. Weißenhofer, U. Nowak, and H. Ebert, Angular momentum transfer via relativistic spin-lattice coupling from first principles, *Phys. Rev. Lett.* **129**, 067202 (2022).
- [20] T. Rudolf, C. Kant, F. Mayr, J. Hemberger, V. Tsurkan, and A. Loidl, Spin-phonon coupling in antiferromagnetic chromium spinels, *New J. Phys.* **9**, 76 (2007).
- [21] M. Ganzhorn, S. Klyatskaya, M. Ruben, and W. Wernsdorfer, Strong spin-phonon coupling between a single-molecule magnet and a carbon nanotube nanoelectromechanical system, *Nat. Nanotechnol.* **8**, 165 (2013).
- [22] I. Paul, Magnetoelastic quantum fluctuations and phase transitions in the iron superconductors, *Phys. Rev. Lett.* **107**, 047004 (2011).
- [23] T. V. Brinzari, J. T. Haraldsen, P. Chen, Q.-C. Sun, Y. Kim, L.-C. Tung, A. P. Litvinchuk, J. A. Schlueter, D. Smirnov, J. L. Manson, J. Singleton, and J. L. Musfeldt, Electron-phonon and magnetoelastic interactions in ferromagnetic, *Phys. Rev. Lett.* **111**, 047202 (2013).
- [24] D. Bossini, M. Pancaldi, L. Soumah, M. Basini, F. Mertens, M. Cinchetti, T. Satoh, O. Gomony, and S. Bonetti, Ultrafast amplification and nonlinear magnetoelastic coupling of coherent magnon modes in an antiferromagnet, *Phys. Rev. Lett.* **127**, 077202 (2021).
- [25] F. Tavazza, D. P. Landau, and J. Adler, Phase diagram and structural properties for a compressible Ising ferromagnet at constant volume, *Phys. Rev. B* **70**, 184103 (2004).
- [26] D. P. Landau, F. Tavazza, and J. Adler, Monte Carlo simulations of a compressible Ising ferromagnet at constant volume, *Comput. Phys. Commun.* **169**, 149 (2005).
- [27] P. Doye, A. A. Louis, I.-C. Lin, L. R. Allen, E. G. Noya, A. W. Wilber, H. C. Kok, and R. Lyus, Controlling crystallization and its absence: proteins, colloids and patchy models, *Phys. Chem. Chem. Phys.* **9**, 2197 (2007).
- [28] T. Huang, Y. Han, and Y. Chen, Melting and solid-solid transitions of two-dimensional crystals composed of Janus spheres, *Soft Matter* **16**, 3015 (2020).
- [29] T. Huang, C. Zeng, H. Wang, Y. Chen, and Y. Han, Internal-stress-induced solid-solid transition involving orientational domains of anisotropic particles, *Phys. Rev. E* **106**, 014612 (2022).
- [30] L. Wan, H. Tao, Y. Tian, C. Zeng, and B. Li, Effect of anisotropic interactions on the heat conduction of one-dimensional chains, *New J. Phys.* **25**, 123021 (2023).
- [31] J. Tobochnik and G. V. Chester, Monte Carlo study of the planar spin model, *Phys. Rev. B* **20**, 3761 (1979).
- [32] P. Olsson, Monte carlo study of the Villain version of the fully frustrated XY model, *Phys. Rev. B* **55**, 3585 (1997).
- [33] J. F. Yu, Z. Y. Xie, Y. Meurice, Y. Liu, A. Denbleyker, H. Zou, M. P. Qin, J. Chen, and T. Xiang, Tensor renormalization group study of classical XY model on the square lattice, *Phys. Rev. E* **89**, 013308 (2014).
- [34] L. Vanderstraeten, B. Vanhecke, A. M. Läuchli, and F. Verstraete, Approaching the Kosterlitz-Thouless transition for the classical XY model with tensor networks, *Phys. Rev. E* **100**, 062136 (2019).
- [35] Y. Zhao, Q. Wu, Q. Chen, and J. Wang, Molecular self-assembly on two-dimensional atomic crystals: Insights from molecular dynamics simulations, *J. Phys. Chem. Lett.* **6**, 4518 (2015).
- [36] R. L. Davidchack, R. Handel, and M. V. Tretyakov, Langevin thermostat for rigid body dynamics, *J. Chem. Phys.* **130**, 234101 (2009).
- [37] G. N. Milstein and M. V. Tretyakov, *Stochastic Numerics for Mathematical Physics* (Springer, Berlin, 2004), Vol. 39.
- [38] E. H. Boubcheur, P. Massimino, and H. T. Diep, Effects of magnetoelastic coupling: critical behavior and structure deformation, *J. Magn. Magn. Mater.* **223**, 163 (2001).
- [39] I. Stockem, A. Bergman, A. Glensk, T. Hickel, F. Körmann, B. Grabowski, J. Neugebauer, and B. Alling, Anomalous phonon life time shortening in paramagnetic caused by spin-lattice coupling: A combined spin and *ab initio* molecular dynamics study, *Phys. Rev. Lett.* **121**, 125902 (2018).
- [40] M. Lapine, I. V. Shadrivov, D. A. Powell, and Y. S. Kivshar, Magnetoelastic metamaterials, *Nat. Mater.* **11**, 30 (2012).
- [41] Y. Liu, N. Lei, W. Zhao, W. Liu, A. Ruotolo, H.-B. Braun, and Y. Zhou, Chopping skyrmions from magnetic chiral domains with uniaxial stress in magnetic nanowire, *Appl. Phys. Lett.* **111**, 022406 (2017).
- [42] Z. Li, Y. Zhang, Y. Huang, C. Wang, X. Zhang, Y. Liu, Y. Zhou, W. Kang, S. C. Koli, and N. Lei, Strain-controlled skyrmion creation and propagation in ferroelectric/ferromagnetic hybrid wires, *J. Magn. Magn. Mater.* **455**, 19 (2018).
- [43] W. Jiang, P. Upadhyaya, W. Zhang, G. Yu, M. B. Jungfleisch, F. Y. Fradin, J. E. Pearson, Y. Tserkovnyak, K. L. Wang, O. Heinonen, S. G. E. Te Velthuis, and A. Hoffmann, Blowing magnetic skyrmion bubbles, *Science* **349**, 283 (2015).